Open Ocean Tide Modelling

M. E. Parke
NRC Associate, NOAA/PMEL, Seattle, Washington 98105

Abstract. The period since the first GEOP conference in 1972 has seen marked changes in global tidal modelling, with many new models produced in the past two years. Two trends have been evident. The first centers on the incorporation of terms for ocean loading and gravitational self attraction into Laplace's Tidal Equations (LTE). The second centers on a better understanding of the problem of near resonant modelling and the need for realistic maps of tidal elevation for use by geodesists and geophysicists. These trends are described. Although new models still show significant differences, especially in the South Atlantic, there are significant similarities in many of the world's oceans. This allows suggestions to be made for future locations for bottom pressure guage measurements. Where available, estimates of M2 tidal dissipation from the new models are significantly lower than estimates from previous models. The new estimates are consistent with recent estimates of the rate of decelleration of the lunar longitude.

Introduction

Over the past seven years since the first GEOP conference in 1972 there have been two marked trends in tidal modelling. The first centers on the incorporation of the terms for ocean loading and gravitational self attraction into Laplace's Tidal Equations (LTE). The second centers on a better understanding of the problem involved with near resonant modelling and the need for realistic maps of tidal elevation for use by geophysicists and geodesists. It is the purpose of this article to describe these two trends, and to look at what improvements are likely in the future.

Because of the scope of the article, and since many researchers have calculated models only for M2, only M2 models after 1972 will be presented. Calculations for other constituents will be mentioned in passing. For a good summary of modelling prior to 1977 and a detailed discussion of modelling techniques see Hendershott [1977]. Another excellent summary can be found in Cartwright [1977].

Ocean Loading and Self Gravitation

The terms for ocean loading and self attraction were incorporated into LTE by Hendershott [1972]. The effect that these terms have on LTE may be summarized as follows. LTE may be written after Hendershott [1977] as a single elliptic elevation equation in negative mercator coordinates as

$$\mathcal{L}(\zeta_o) + \varepsilon^2 \mathrm{sech}^2\tau\, \zeta_o = \mathcal{L}(\Gamma/g-\delta) + \overline{F} \qquad (1)$$

where

$$\mathcal{L} = QH\nabla^2 + [(QH)_\phi - (i/s)(QH\tanh\tau)_\tau]\partial\phi + [(QH)_\tau + (i/s)(QH\tanh\tau)_\phi]\partial\tau \qquad (2)$$

$$\overline{F} = (1/\rho D_o)[(QF^\phi)_\phi + (QF^\tau)_\tau] - (i/\rho D_o s)[(Q\tanh\tau F^\phi)_\tau - (Q\tanh\tau F^\tau)_\phi] \qquad (3)$$

and

$$\varepsilon^2 = 4\Omega^2 a/gD_o \qquad Q = 1/(s^2-\tanh^2\tau)$$
$$D = D_o H(\phi,\tau) \qquad s = \sigma/2\Omega \qquad (4)$$

where τ,ϕ are the mercator latitude and longitude, ζ_o is the observed ocean tide, F^τ, F^ϕ are the meridional and zonal components of dissipative stress, σ is the tidal forcing frequency, Ω is the earth's angular rate of rotation, Γ is the total tide generating potential, δ is the geocentric solid earth tide, D is the local depth of the ocean, and a is the radius of the earth. The exact form of dissipative stress for each model will depend on the choice of F^τ and F^ϕ.

For a rigid earth, $\Gamma = U$ (the astronomical potential) and $\delta = 0$, i.e.

$$\Gamma/g - \delta = U/g \qquad (5)$$

In the presence of solid earth deformation and tidal loading $\Gamma/g - \delta$ may be expressed as follows. In the usual Love number notation (Munk and MacDonald, 1960, p. 24,29,30), the n^{th} spherical harmonic component of the potential is

$$\Gamma_n = (1+k_n)U_n + (1+k_n')g\alpha_n\zeta_{on} \qquad (6)$$

while the n^{th} spherical harmonic component of the solid earth tide is

$$\delta_n = h_n U_n/g + h_n'\alpha_n\zeta_{on}. \qquad (7)$$

Here the n^{th} spherical harmonic of the observed ocean tide is

$$\zeta_{on} = \sum_m C_{nm} Y_n^m(\sin\theta) \qquad (8)$$

where Y_n^m is the spherical harmonic normalized after Backus [1958], i.e. $|Y_n^m| = 1$, U_n is the n^{th} spherical harmonic component of the astronomical potential (in practice only U_2 need be considered), θ is the latitude, and

$$C_{nm} = \iint \zeta_o(\phi',\theta') Y_n^m(\sin\theta')\cos\theta'\,d\phi'\,d\theta'. \qquad (9)$$

Thus if one defines

$$\overline{\zeta} = \sum_n (1+k_n-h_n)U_n/g \qquad (10)$$

then

$$\Gamma/g - \delta = \overline{\zeta} + \sum_n (1+k_n'-h_n')\alpha_n \iint \zeta_o Y_n^{m*}\cos\theta'\,d\phi'\,d\theta' \qquad (11)$$

Proc. of the 9th GEOP Conference, *An International Symposium on the Applications of Geodesy to Geodynamics, October 2-5, 1978*. Dept. of Geodetic Science Rept. No. 280. The Ohio State Univ., Columbus, Ohio 43210.

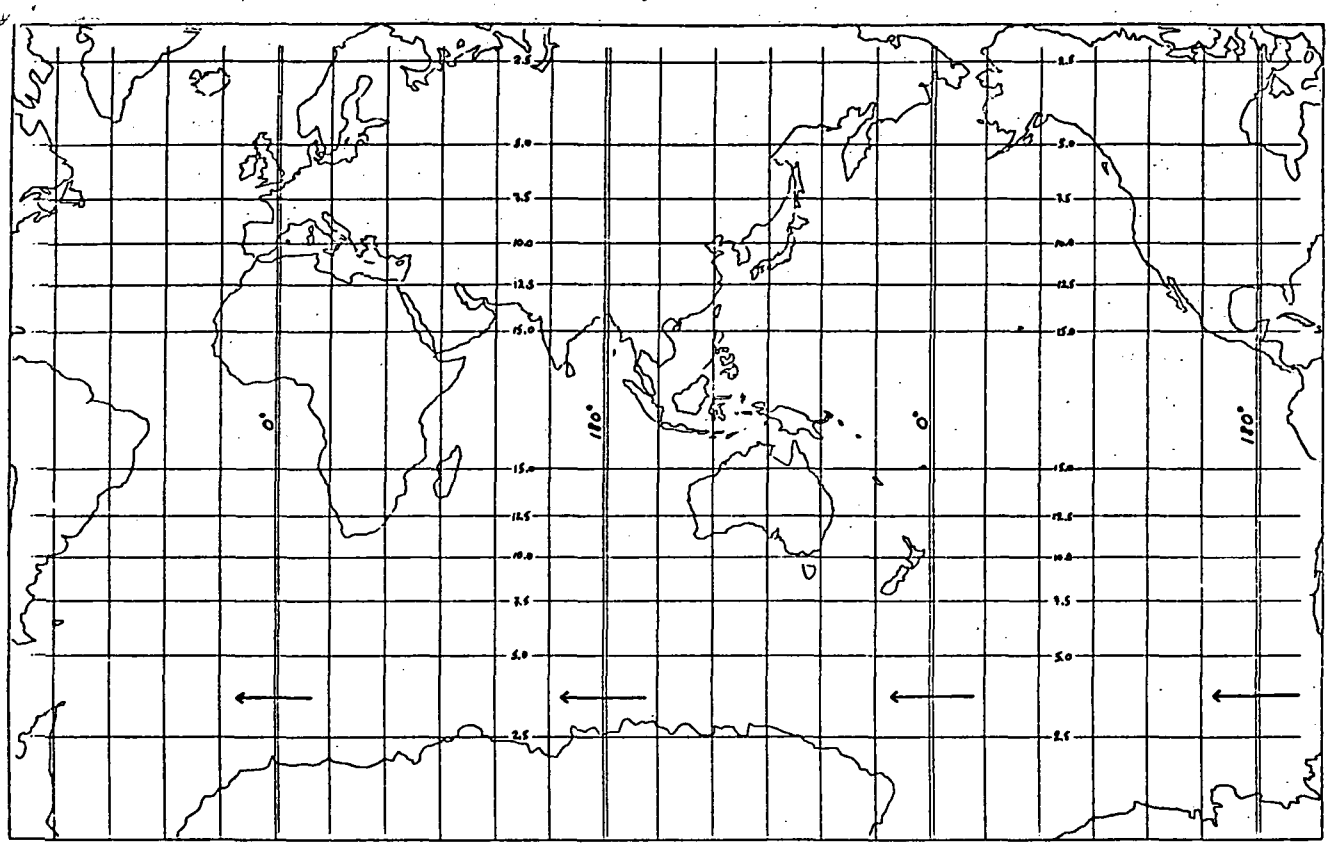

Fig. 1. The M2 gravitational potential divided by g seen by an observer fixed to the surface of the earth in the absence of ocean tidal effects, i.e. $(1+k_2-h_2)U_2$. (amplitudes in cm, phases in degrees)

or by placing the summation inside the integral,

$$\Gamma/g - \delta = \overline{\zeta} + \iint \zeta_o(\phi',\theta')G(\phi',\theta'|\phi,\theta)\cos\theta' d\phi' d\theta' \quad (12)$$

where $G(\phi',\theta'|\phi,\theta)$ is a Green's function evaluated by Farrell [1972]. In negative mercator coordinates

$$\Gamma/g - \delta = \overline{\zeta} + \iint \zeta_o(\phi',\tau')G(\phi',\tau'|\phi,\tau)\mathrm{sech}^2\tau' d\phi' d\tau' \quad (13)$$

The presence of this global integral makes solution difficult. Hendershott [1972] proposed the iterative sequence

$$\mathcal{L}(\zeta_o^1) + \varepsilon^2\mathrm{sech}^2\tau\zeta_o^1 = \mathcal{L}(\textstyle\sum_n(1+k_n-h_n)U_n/g) + \overline{F} \quad (14)$$

$$\mathcal{L}(\zeta_o^i) + \varepsilon^2\mathrm{sech}^2\tau\zeta_o^i = \mathcal{L}(\textstyle\sum_n(1+k_n-h_n)U_n/g) + \overline{F} + \iint \zeta_o^{i-1}G(\phi',\tau'|\phi,\tau)\mathrm{sech}^2\tau' d\phi' d\tau' \quad (15)$$

and found it divergent for M2 in the absence of interior dissipation, i.e. $\overline{F} = 0$. Gordeev, et. al [1977] showed that this procedure will converge in the presence of interior dissipation. Their calculations based on the Longman [1963] Green's function are consistent with the importance of these terms. Parke [1978a] showed dramatically that the loading and self gravitation terms are important for M2 by comparing the surface potential seen by an observer fixed to the surface of the earth with and without ocean effects, i.e.

$$\Gamma/g = (1+k_2-h_2)U_2/g \quad (16)$$

vs

$$\Gamma/g = (1+k_2-h_2)U_2/g + \textstyle\sum_n(1+k_n'-h_n')\alpha_n\zeta_{on} \quad (17)$$

where the ocean terms were calculated based on the Parke-Hendershott model discussed in the next section. These charts are shown in figures 1 and 2. Note the considerable distortion in the North Atlantic caused by the ocean effects. Historically researchers have had trouble with local models of the North Atlantic using the equilibrium potential. Perhaps this is the reason why.

Over the past several years the importance of the terms for ocean loading and self attraction has gradually become accepted, with models sans ocean loading effects being published as late as 1977. Starting in 1972, the first iteration of Hendershott is a model sans loading effects and is presented in figure 3. The calculation is based on a six degree Mercator grid with specified elevation boundary conditions and implicit dissipation, i.e. $\overline{F} = 0$. Energy is allowed to freely flow through the boundaries to be dissipated in the shallow seas and shelves.

Zahel [1973] calculated a model for K1 using a four degree spherical mesh graded toward the

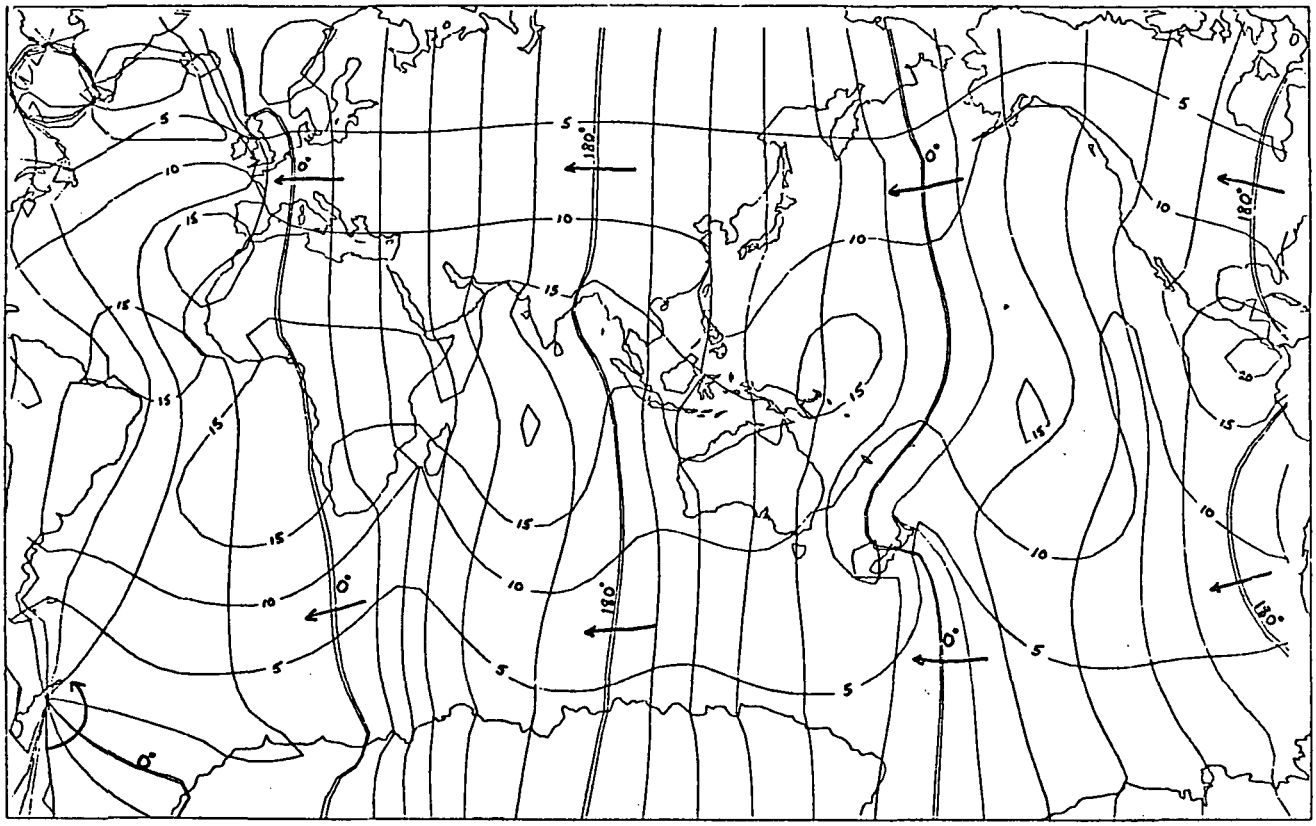

Fig. 2. The M2 gravitational potential divided by g seen by an observer fixed to the surface of the earth when the effects of ocean loading and gravitational self attraction from the Parke-Hendershott [1978] tidal model are added, i.e. $(1+k_2-h_2)U_2 + \sum_n (1+k_n'-h_n')\alpha_n \zeta_{on}$. (amplitudes in cm, phases in degrees)

poles, reflecting boundary conditions, and dissipation of the form

$$F/\rho D = -r((u^2+v^2)^{1/2}/D)\underline{u} + AV^2\underline{u} \qquad (18)$$

where r is a bottom drag coefficient and A a lateral eddy viscosity with r = .003 and A = 10^7 cm^2/sec. Zahel presented a similar calculation for M2 on a one degree mesh at the IUGG meeting in Grenoble in 1975, and subsequently published [Zahel,1977]. Figure 4 is a copy of the cotidal chart presented in 1975. Zahel has recently completed a model including loading effects (Trevor Baker, personnal communication).

Estes [1977] repeated Zahel's procedure for M2 using a two degree mesh and allowing for deformation of the solid earth by the astronomical forcing. Resulting amplitudes were smaller as would be expected. This calculation was extended to S2, N2,K2,K1,O1, and P1. The M2 model was used as a starting point for the iterative procedure of Hendershott described above. Convergence was found after 16 iterations. This model is shown in figure 5.

Parke [1978b] solved the modified LTE on a six degree Mercator mesh using specified elevation boundary conditions and no interior dissipation. This was done by using a set of test functions similar to the iterates of Hendershott as a basis set for a least squares fit to the complete equations. The test functions were generated by the same method as the iterates, except that periodically the best least squares fit was subtracted from the equations and an iterative sequence started on the residuals. This was done to aid numerical stability. Solutions for M2 and S2 were found to be unrealistically resonant, while for K1 the iterative procedure of Hendershott was found to be convergent and the solution showed every sign of being far from resonance.

Accad and Pekeris [1978] calculated models for M2 and S2 using a two degree mercator mesh with implicit dissipation determined at the coasts by a modified Proudman boundary condition. Instead of treating the edge of the coastal shelves as a step function, they treat it as a linear ramp. For a step function, the assumption that the energy contained in the upper layer (of depth h') is dissipated rather than reflected leads to the usual Proudman condition

$$hu_n = (gh')^{1/2}\zeta_o \qquad (19)$$

where h is the depth offshore from the shelf and u_n is the normal velocity. When the edge of the shelf is considered as a ramp, this condition becomes

$$hu_n = (gh)^{1/2}(1-R)/(1+R)\zeta_o \qquad (20)$$

where R is a complex reflection coefficient depending on S (the width of the ramp), h, and h'. Accad and Pekeris used the values S = 100km and h' = 10m, while h was taken to be the observed

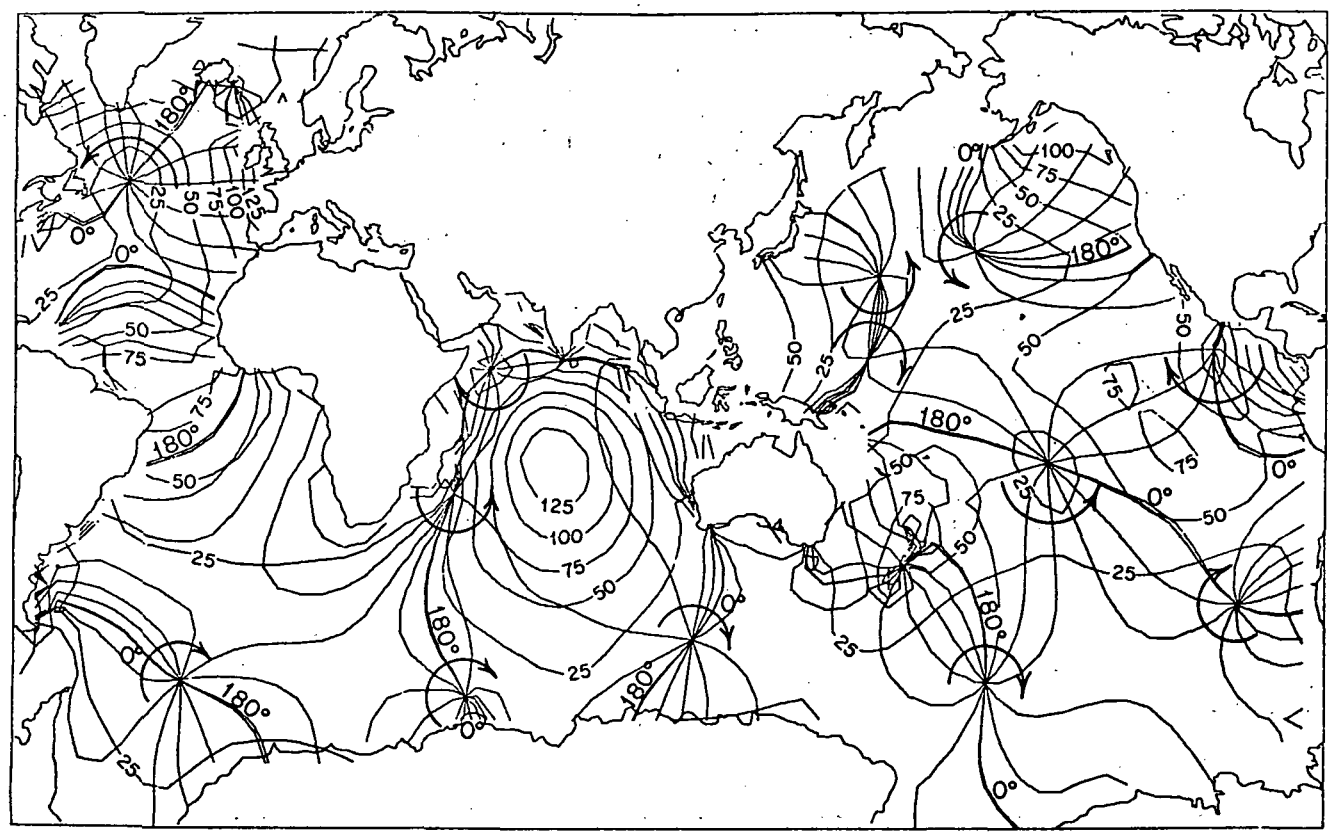

Fig. 3. The Hendershott [1972] M2 tidal model. (amplitudes in cm, phases in degrees)

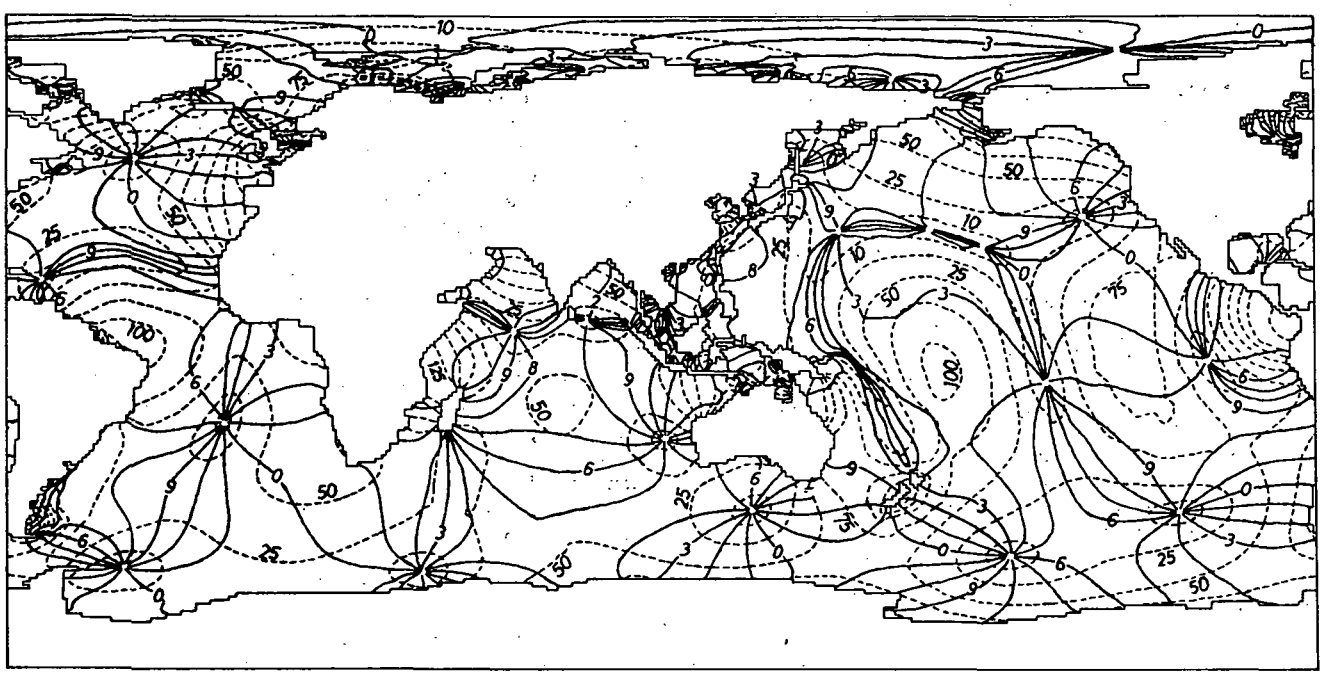

Fig. 4. The Zahel [1977] M2 tidal model. (amplitudes in cm, phases in lunar hours)

value of the ocean depth closest to the grid point on the coast. Ocean loading terms were approximated by

$$\sum_n (1+k'_n-h'_n)\alpha_n \zeta_{on} \simeq 0.085\zeta_o \simeq \sum_n 0.085\zeta_{on} \qquad (21)$$

or

$$(1+k'_n-h'_n)\alpha_n \simeq 0.085 \qquad (22)$$

for all n. The M2 results are given in figure 6.

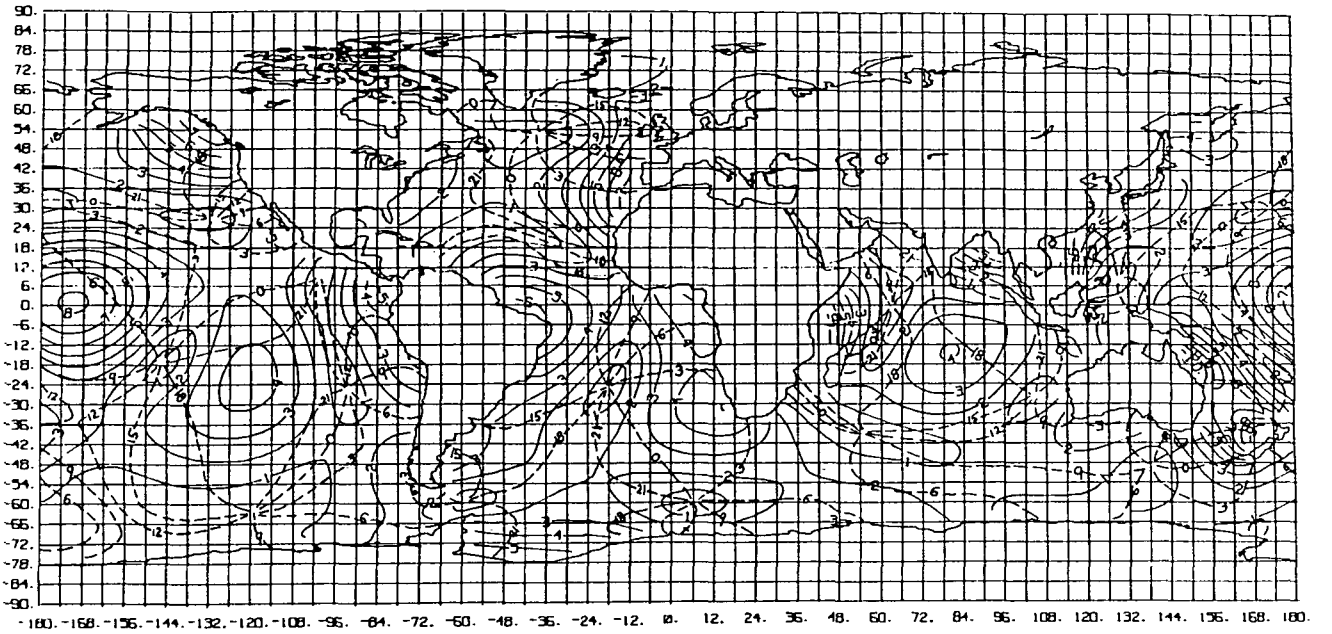

Fig. 5. The Estes [1977] M2 tidal model with the effects of ocean loading and self attraction included. (amplitudes in decimeters, phases in lunar half hours)

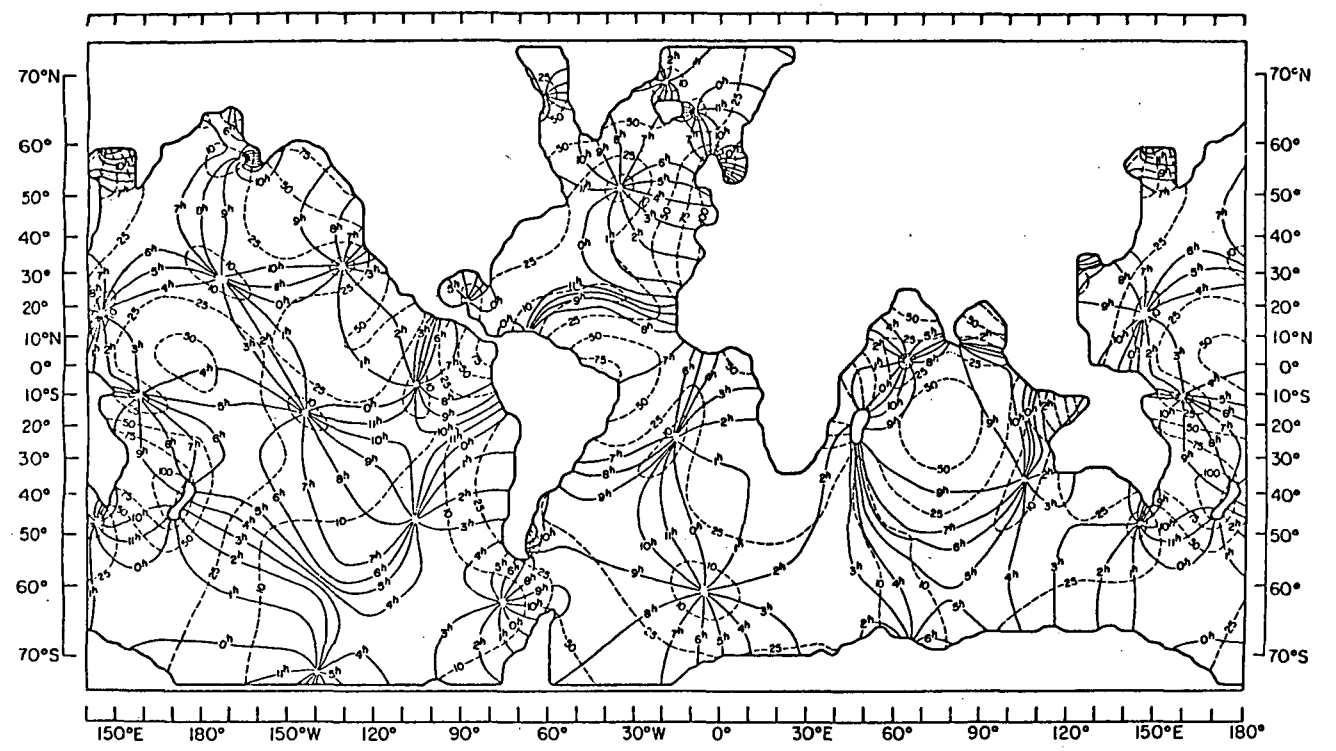

Fig. 6. The Accad and Pekeris [1978] M2 tidal model. (ampl. in cm, phases in lunar hours)

Near Resonant Modelling

Over the past few years there has been increasing geophysical interest in finding a realistic representation of the open ocean tide. Historical models of the semi-diurnal tides (primarily M2) show significant differences, especially in the Pacific and South Atlantic. Considering the closeness to resonance of the problem, though, the level of agreement is actually quite remarkable. The fact that there are significant differences, however, means that to produce realistic maps of the ocean tidal elevation the problem of resonance must be handled. This problem arises because small errors in how one's model represents the real ocean basins cause small errors in the frequencies at which the model basin resonates. Near resonance this causes a significant error in the assigned amplitudes for these modes.

As an example of a near resonant one mode sys-

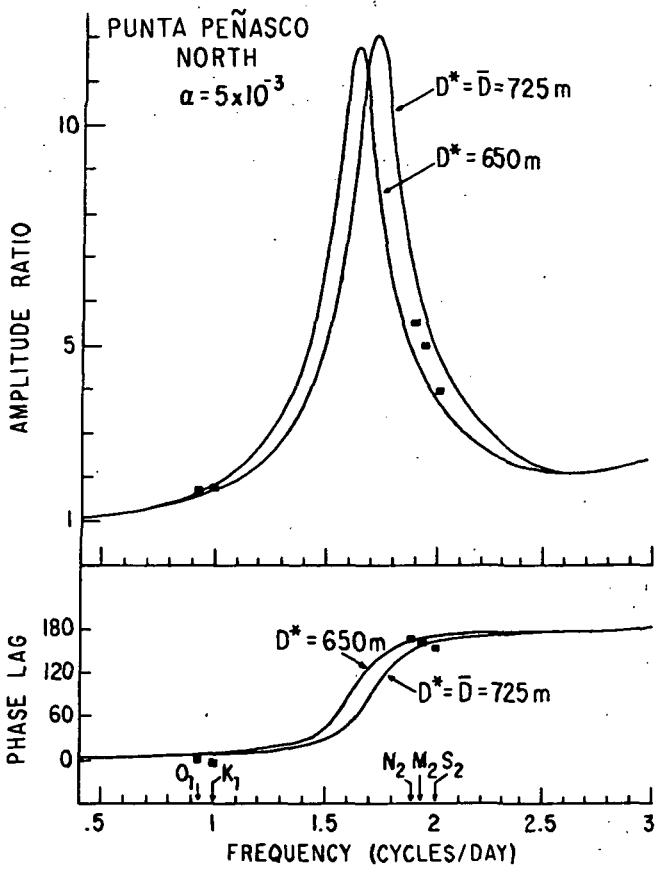

Fig. 7. A comparison of the tidal response at Punta Peñasco North to the tide at the mouth of the Gulf of California for two models with different mean depth, after Stock [1976].

tem, figure 7 shows the model response of the Gulf of California at two different mean depths after Stock [1976]. Far from resonance, e.g. O1 and K1, the difference between the responses is small. Near resonance, however, e.g. for M2, S2, and N2, the difference is quite significant. In a one mode system such as the Gulf of California, this effect can be adjusted with a single parameter such as the mean depth. The global tide, however, appears to be more complex. Four possible approaches are:

(1) If one knew the near resonant global normal modes, one could adjust one's model accordingly.

(2) One can adjust model parameters. Schwiderski [1978] follows this approach with a one degree graded spherical mesh with linear eddy dissipation with eddy viscosity A given by

$$A = aH(\lambda,\phi)L/2(1+\mu\cos\phi) \qquad (23)$$

and a linear bottom friction term with coefficient

$$B = bL^2\mu\cos\phi \qquad (24)$$

where a and b are trial and error parameters, L is the equatorial mesh size, μ is the mesh grading parameter, and $H(\lambda,\phi)$ is the local depth of the ocean. Note that A is directly proportional to H, and that B has no depth dependence. The linear bottom friction term is adjusted within set limits at each boundary point and island station to force as close as possible agreement between the observed and calculated tides at these locations. Loading terms are approximated after Pekeris by

$$\sum_n (1+k'_n-h'_n)\alpha_n\zeta_{on} \simeq 0.1\zeta_o \qquad (25)$$

where the factor 0.1 is attributed to Pekeris. A cotidal chart copied from a plot provided by Ron Estes is shown in figure 8. One consequence of forcing agreement at island stations is the creation of small scale local distortions. See for example the Southwest Pacific.

(3) Parke and Hendershott [1978] took the set of test functions used by Parke [1978b] to solve the modified LTE in the absence of interior dissipation and fit them in the least squares sense to interior (island) data. This was done for M2, S2, and K1 and represents a first order correction to the problem. The resulting models are on a six degree Mercator mesh with specified elevation boundary conditions and dissipation only in shallow seas and on shelves. Encouraging is the fact that the M2 calculation was shown to be stable over a ±5% variation in the mean depth. All three representations conserve mass. A cotidal chart for M2 is given in figure 9.

(4) Estes (personnal communication) proposes combining models of the tide with other data such as altimetry and gravity measurements, with the model value at each point considered simply as another datum.

It is interesting and provocative that the Schwiderski and Parke-Hendershott models show many qualitative and quantitative similarities throughout much of the worlds oceans. Starting with the Pacific, both show a convergence of phases between Japan and New Guinea, amphidromes off California, Latin America, Chile, and in the Central Pacific. West of the California amphidrome Schwiderski shows small amplitudes and a convergence of phases, while Parke-Hendershott shows a double amphidrome. It should be noted that the absolute difference between these two cases is small. The amphidrome that Parke-Hendershott show southeast of New Zealand has moved much farther to the east and south in the Schwiderski model. Both show two anti-amphidromes in the Pacific; Parke-Hendershott at approximately 4°N 174°E and 2°S 126°W while Schwiderski places them at approximately 6°S 176°E and 4°S 129°W. The dominant feature of the Indian Ocean for all models is a central anti-amphidrome. Parke-Hendershott place this at approximately 18°S 78°E while Schwiderski places it at approximately 20°S 78°E. In the South Atlantic Parke-Hendershott show a region of low amplitudes extending eastward from South America while Schwiderski shows a double amphidrome. Both show an anti-amphidrome next to the tip of Africa with Parke-Hendershott placing it at approximately 32°S 5°E and Schwiderski at 30°S 10°E.

Discussion

Table 1 summarizes the global tide models calculated since 1972. Recent estimates of model dissipation by Parke-Hendershott [1978] of 2.22 x 10^{19} ergs/sec and by Accad and Pekeris of 2.55 x

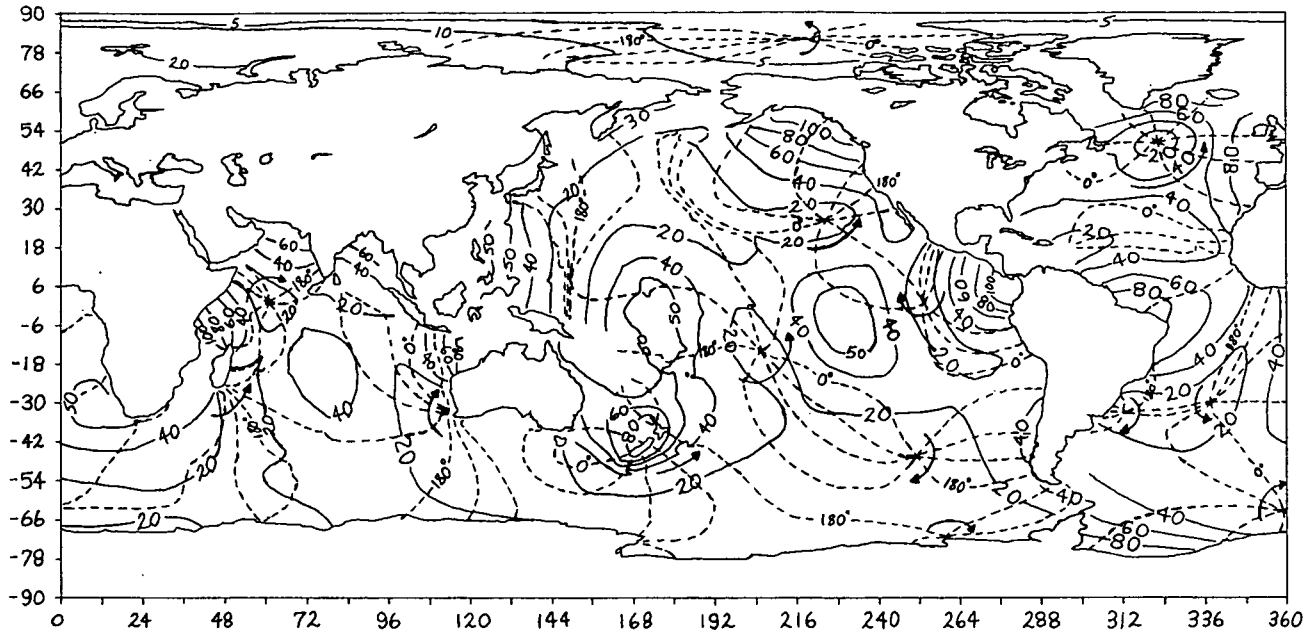

Fig. 8. The Schwiderski [1978] M2 tidal model. Many shallow seas and shelves such as the Patagonian shelf show spacial structure much too fine to be resolved at these scales and so these regions have been left blank. (amplitudes in cm, Phases in degrees)

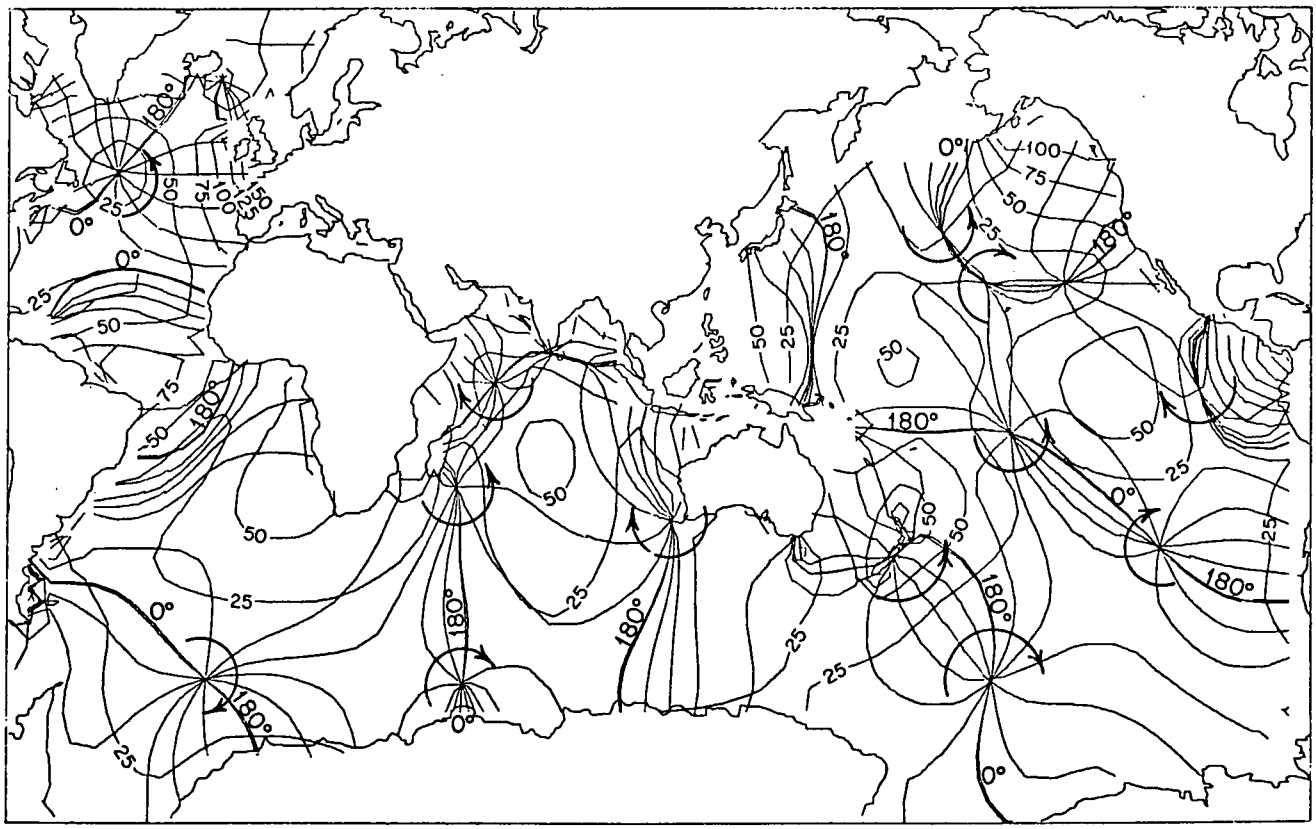

Fig. 9. The Parke-Hendershott [1978] M2 tidal model. (amplitudes in cm, phases in degrees)

10^{19} ergs/sec are significantly lower than previous model estimates. Recent astronomical estimates include Muller [1977] with 3.3 ± .2 x 10^{19} ergs/sec and Goad and Douglas [1978] with 3.3 ± .4 x 10^{19} ergs/sec. It should be noted that the astronomical estimates are for all lunar dissipations not just M2. Estimates of the non-M2 ocean contribution to lunar dissipation vary from 0.3 - 1.0 x 10^{19} ergs/sec. This leaves a range for the M2 ocean tidal dissipation based on the Muller estimate of 2.1 - 3.2 x 10^{19} ergs/sec. Miller [1966] estimates empirically a M2 dissipation in the shallow seas and shelves of 0.9 - 2.5 x 10^{19} ergs/sec. Combining these two esti-

TABLE 1: Summary of Global Ocean Tidal Models since 1972

Model	Constituent(s)	Mesh	Boundary Conditions	Form of Dissipation	Dissipation ($\times 10^{19}$ erg s^{-1})	Loading Terms
Hendershott [1972]	M2	6° mercator	specified elevation	implicit, in shallow seas and shelves only	3.08	yielding to astronomical force only
Zahel [1973]	K1	4° spherical	reflecting	bottom stress in shallow water	-	none
Zahel [1973]	M2	1° spherical	reflecting	bottom stress in shallow water	3.77	none
Estes [1977]	M2,S2,N2,K2, K1,O1,P1	2° spherical	reflecting	bottom stress in shallow water	-	yielding to astronomical force only
Estes [1977]	M2	3° spherical	reflecting	bottom stress in shallow water	-	complete potential using Green's function
Schwiderski [1978]	M2	1° spherical	reflecting	bottom friction $bL^2\mu\cos\phi$ eddy dissipation $a/2\ L\ H(\lambda,\phi)(1+\mu\cos\phi)$	-	estimate loading terms with $0.1\zeta_o$
Parke-Hendershott [1978]	M2,S2,K1	6° mercator	specified elevation	implicit, in shallow seas and shelves only	M2 = 2.22 S2 = 0.208 K1 = 0.221	complete potential using Green's function
Accad and Pekeris [1978]	M2,S2	2° mercator	modified Proudman condition using ramp shaped shelf edge	implicit, in shallow seas and shelved only	M2 = 2.55 S2 = 0.526	estimate loading terms with $0.085\zeta_o$

mates, one would expect M2 ocean tidal dissipation to be in the range 2.1 - 2.5 x 10^{19} ergs/sec which is in excellent agreement with the new model estimates.

In the last section, it was noted that there exists a marked similarity between the models of Parke-Hendershott and Schwiderski. There are also a number of qualitative similarities with the loading solutions of Estes and Accad and Perkeris. All four models show two anti-amphidromes in the Pacific and one in the Indian Ocean, although Estes' anti-amphidrome in the eastern Pacific is much further south than that for the other three. Estes also shows an anti-amphidrome just west of the tip of Africa similar to that of Parke-Hendershott and Schwiderski. All four show amphidromes in the North Atlantic, in the South Atlantic near Antartica, off the coast of California, and in the central Pacific.

Anti-amphidromes represent ideal places for bottom pressure guage measurements, since they are locations of large ampitude and spacial stability. Because of the strong similarities in the location and number of anti-amphidromes in the above M2 models, a strong recommendation can be made as to where measurements should be taken. Thus the following list of locations is recommended; near 1°S 175°E, near 3°S 128°W, near 19°S 78°E, and near 31°S 8°E. Also since there are relatively large variations from model to model in the South Atlantic between South America and Africa, 30°S 30°W is recommended.

Although new models for other constituents are not shown here, similar recommendations can be made for S2. Accad and Pekeris' S2 model shows anti-amphidromic points at 2°N 176°E, 10°N 142°W, and 18°S 74°E while Parke-Hendershott show anti-amphidromic points at 6°N 172°E, 8°N 142°W, and 22°S 75°E. Therefore ideal locations for S2 bottom pressure guage measurements would be at 4°N 174°E, 9°N 142°W, and 20°S 74°E. Not surprisingly, two of the three locations are almost identical with those for M2.

For the future, there are three potential directions for improvement in the ability to represent the open ocean tide. All models refer back to known observations either directly through specified elevation boundary conditions, indirectly through adjustment of a friction parameter(s), or simply as a measure of model quality. Unfortunately, coastal observations are on the wrong side of the shelves, and quite often in bays or estuaries. Island observations are often inside lagoons. The growing collection of bottom pressure guage measurements will help. Cartwright and Zetler (personnel communication with Zetler) are collecting present measurements for publication by the International Association for the Physical Sciences of the Ocean (IAPSO). Shelf models of such difficult regions as the Patagonian Shelf will also help. Satellite altimetry measurements will ultimately provide spacial (if not as accurate) coverage of the global tide. In special regions where there are high tidal amplitudes and short length scales, so that the spacial structure of the tide can be separated from orbit errors, existing satellite data can quite possibly be utilized.

Acknowledgements. This paper was developed as part of a research associateship with the National Research Council. The author would like to thank Ron Estes for forwarding a cotidal chart for Schwiderski's model and for forwarding a copy of Accad and Pekeris' preprint.

References

Accad, Y., and C. L. Pekeris, Solution of the tidal equations for the M2 and S2 tides in the world oceans from a knowledge of the tidal potential alone, preprint, Department of Applied Mathematics, the Weizmann Institute, Rehovot, Israel, 1978.

Backus, G., A class of self-sustaining dissipative sperical dynamos, Ann. Phys. (N.Y.),4, 372-447, 1958.

Cartwright, D. E., Oceanic tides, Rep. Prog. Phys., 40, 665-708, 1977.

Estes, R. H., A computer software system for the generation of global ocean tides including self-gravitation and crustal loading effects, X-920-77-82, Goddard Space Flight Center, Greenbelt, Md., 60 pages, 1977.

Farrell, W. E., Deformation of the earth by surface loads, Rev. Geophys. Space Phys., 10, 761-797, 1972.

Goad, C. C., and B. C. Douglas, Lunar tidal acceleration obtained from satellite-derived ocean tide parameters, Jour. Geophys. Res., 83, 2306-2310, 1978.

Gordeev, R., B. Kagan and E. Polyakov, The effects of loading and self attraction on global ocean tides, the model and the results of a numerical experiment, J. Phys. Oceanogr., 7, 161-170, 1977.

Hendershott, M. C., The effects of solid earth deformation on global ocean tides, Geophys. J. Roy. Astron. Soc., 29, 389-402, 1972.

Hendershott, M. C., Numerical models of ocean tides in The Sea, Chapter 6, Goldberg, McCave, O'Brien, Steele eds., Wiley-Interscience, New York, 1977.

Longman, I., A Green's function for determining the deformation of the earth under surface mass loads, Jour. Geophys. Res., 68, 485-496, 1963.

Miller, G., The flux of tidal energy out of the deep oceans, Jour. Geophys. Res., 71 (4), 2485-2489, 1966.

Muller, P., Determination of the rate of change of G and the tidal acceleration of earth and moon from ancient and modern astronomical data, SP43-36, The Jet Propulsion Laboratory, Pasadena, Ca., 24 pages, 1976.

Munk, W.H., and G. MacDonald, The Rotation of the Earth, Cambridge University Press, London, 1960.

Parke, M. E., and M. C. Hendershott, M2,S2,K1 models of the global ocean tide on an elastic earth, Marine Geodesy, in press, 1978.

Parke, M. E., Global modelling of tides on an elastic earth, Proc. Int. Long Wave Symposium, Ottawa, Canada, 1978a.

Parke, M. E., Global numerical models of the open ocean tides M2,S2,K1 on an elastic earth, PhD Thesis, Univ. of California at San Diego, 1978b.

Schwiderski, E. W., Global ocean tides, part I: a detailed hydrodynamical interpolation model, NSWC/DL TR-3866, Naval Surface Weapons Center, Dahlgren, Virginia, 1978.

Stock, G., Modelling of tides and tidal dissipation in the Gulf of California, PhD Thesis, Univ. of California at San Diego, 1976.

Zahel, W., The diurnal K1 tide in the world ocean - a numerical investigation, Pure and Applied Geophysics, 109, viii, 1819-1825,1973.

Zahel, W., Proc. IRIA Int. Colloq. on Numerical Methods of Science and Technical Computation, Berlin: Springer-Verlag, 1977.

Page Intentionally Left Blank